Wideband Octagonal Dual Circularly Polarized Sub-array Antenna for Ku-Satellite Systems

Khalid. M. Ibrahim [1], Walaa. M. Hassan [1], Esmat A. Abdallah [2], and Ahmed M. Attiya [1]

[1] Microwave Engineering Department
Electronics Research Institute, Cairo, Egypt
khaledmus@gmail.com, walaa81hassan@yahoo.com, attiya@eri.sci.eg

[2] Microstrip Department
Electronics Research Institute, Cairo, Egypt
esmataa2@hotmail.com

Abstract ─ In this paper the analysis and design of a dual circularly polarized 4×4 antenna array operating in Ku-band are discussed with emphasis on its sequential feeding network. The dual circular polarization is achieved by feeding a stacked octagonal patches with a wideband branch line coupler. The proposed 4×4 antenna array is based on two separate sequential feeding networks for LH and RH circular polarizations. The advantage of the proposed feeding network is that it is implemented on a single layer. Simulation results by using both HFSS and CST are presented for comparison. In addition, experimental verifications are presented**.**

Index Terms ─ Antenna array, circular polarization, feeding network, satellite antenna, wideband antenna.

I. INTRODUCTION

On-move satellite communication systems at Ku band have a significant importance in different applications where it may not be available other communication systems with similar bandwidth and service stability [1]. These on-move satellite communication systems are quite suitable for vehicles in rural areas, airplanes and ships in rivers and seas. These applications require low profile, low weight, dual polarization and wideband antenna systems. In addition, these antennas should satisfy the ITU requirements to avoid interference with other satellites [2]. The proposed operating frequency range is from 10.5 GHz to 14.5 GHz with dual circular polarizations. Printed antenna arrays with properly tapered feeding network inside radoms are good candidates for these applications. Other configurations based on waveguide antenna array are also found in literature [3]-[5]. However, these configurations have larger weight and less conformity compared to printed antennas like microstrip antennas. Different configurations of printed antenna elements for this frequency band are presented in literature [6]-[8]. However, the main problem lies in developing appropriate feeding network to introduce an antenna array of these radiating elements which sustain wideband and dual polarization properties in addition to the required properties of the radiation pattern. To simplify the feeding network, the antenna array is divided into smaller sub-arrays composed of 4×4 radiating elements. Each sub-array is fed by a uniform distribution network while a master separated non-uniform distribution network is used to feed these sub-arrays [9]. On the other hand, for the case of a circularly polarized antenna array, the axial ratio would be enhanced by using a combination of circularly polarized elements with a sequential feeding network. Implementing this sequential feeding network for a single circular polarization is discussed by using different configurations in [4], [10]-[11]. However, these configurations of sequential feeding networks cannot be used for dual circular polarizations at the same layer. This increases the number of layers in the feeding network for the case of dual circular polarization which increases the cost, weight and manufacturing complexity. Another configuration based on substrate integrated waveguide for dual circular polarization is introduced in [12]. However, this configuration has a limited bandwidth in the range from 11.8 to 13 GHz only. Thus, for the proposed application, it is required to develop a dual sequential feeding network on the same layer for a 4×4 sub-array. A similar antenna configuration is presented in [13] based on multi-layered FSS integrated with AMC structure fed by a double sided dipole array. However, this structure is operating in the Ku-band in the frequency range from 14 to 15.5 GHz only and in the X-band from 7.5 to 8.5 GHz.

The target of the present paper is to design a single layer sequential feeding network for a Ku-band dual

Submitted On: July 27, 2020
Accepted On: November 29, 2020
https://doi.org/10.47037/2020.ACES.J.351207

circularly polarized 4×4 antenna sub-array operating in the frequency range from 10.5 to 14.5 GHz. This sub-array is designed to be integrated in a complete antenna array for on-move satellite communication system. The size of this sub-array is limited to be less than 75×75 mm^2. This limited size increases the complexity of designing dual sequential feeding network on a single layer due to the coupling between the different parts of the feeding network. In addition, the required wide bandwidth, which is nearly 27.5%, represents another important challenge in the design of this feeding network.

The paper is organized as follows: Section II presents analysis and design of a dual circular polarized octagonal radiating element. Section III presents analysis and design of 4×4 sequential fed dual circular polarized antennas. The simulation process are developed by using HFSS ver.14 [14] and verified by using CST ver.2012 [15]. The experimental results are presented in Section IV. Finally, the conclusion is presented in Section V.

II. ANALYSIS AND DESIGN OF DUAL CIRCULAR POLARIZED OCTAGONAL RADIATING ELEMENT

To obtain a wideband operation, stacked microstrip patch antenna configuration is proposed to be the radiating element of this antenna array as shown in Fig. 1 (a). The bandwidth of this stacked configuration can be enhanced by introducing an electrically thick layer of a low dielectric material between the fed element and the parasitic element. Foam is a quite suitable material for this purpose where its dielectric constant is around 1.07. The key parameters in the design of this wideband radiating element are the substrate parameters of the fed element, the dimensions of the fed element, the dimensions of the parasitic element, the separation between the fed element and the parasitic element, and the parameters of the superstrate which holds the parasitic element. The proposed geometry of the fed and parasitic elements in the present antenna are octagonal shape as shown in Figs. 1 (b).

The substrate of the fed element is a grounded Rogers 5880 with a dielectric constant $\varepsilon_r = 2.2$, $\tan\delta = 0.0009$ and dielectric thickness $L_2 = 0.787$mm. The parasitic element is printed on RO3003 substrate of a thickness $L_1 = 0.25$ mm. The dielectric constant of this substrate is 3 and its loss tangent is 0.001. The two substrates are separated by a foam layer of thickness $L_F = 2$ mm.

The analysis of this antenna configuration starts with approximate circular patches to obtain approximate dimensions of the fed patch and the parasitic patch. Then these approximate dimensions are tuned by using numerical electromagnetic simulation tools like HFSS and CST to obtain the required operating bandwidth.

The resonant frequency of TM_{110} mode for a circular patch antenna on the lower substrate can be obtained by using cavity model as following [17]:

$$f_0 = \frac{1.841c}{2\pi a_e\sqrt{\varepsilon_r}}, \tag{1}$$

where a_e is the effective radius taking into account the fringing effect. This effective radius is given by:

$$a_e = a\sqrt{1+\frac{2h}{\pi a\varepsilon_r}\left[\ln\left(\frac{\pi a}{2h}\right)+1.7726\right]}. \tag{2}$$

For design purpose, the radius of a circular microstrip antenna which would be resonant at frequency f_0 can be obtained as follows:

$$a = \frac{F}{\sqrt{1+\frac{2h}{\pi\varepsilon_r F}\left[\ln\left(\frac{\pi F}{2h}\right)+1.7726\right]}} \text{ cm}, \tag{3}$$

where

$$F = \frac{8.791\times10^9}{f_0\sqrt{\varepsilon_r}}. \tag{4}$$

On the other hand, the resonance of the upper patch is obtained by using an equivalent relative permittivity given by:

$$\varepsilon_{ef} = \frac{4\varepsilon_{re}\varepsilon_{r,dyn}}{\left(\sqrt{\varepsilon_{re}}+\sqrt{\varepsilon_{r,dyn}}\right)^2}, \tag{5}$$

where

$$\varepsilon_{re} = \frac{\varepsilon_r\left(1+L_f/L_2\right)}{\left(1+\varepsilon_r L_f/L_2\right)}, \tag{6}$$

and

$$\varepsilon_{r,dyn} = \frac{C_{dyn}(\varepsilon=\varepsilon_0\varepsilon_{re})}{C_{dyn}(\varepsilon=\varepsilon_0)}, \tag{7}$$

where C_{dyn} is the dynamic capacitance. The details of calcualting $\varepsilon_{r,dyn}$ can be found in [18].

Based on th above analysis, the intial designs of the lower and the upper patches are obtained as circular patches with radii $R_1 = 4.1\,mm$ and $R_2 = 4.4\,mm$ respectively. These radii are corresponding to resonant frequencies 13 GHz and 12 GHz respectively to enable operation from 10.5 GHz to 14.5 GHz. These initial dimensions are then cut in octagonal shapes as shown in Fig. 1 (b) to tune the matching of this antenna structure to the required operating band. This adjustment is done numerically by using numerical simulation tools.

On the other hand, a dual circular polarized antenna can be obtained by developing a dual feeding network which introduces two simultaneous feeding points of equal amplitudes and phase shifts of $\pm90^o$. Quadrature branch-line coupler (BLC) is a quite appropriate candidate for this application. However, conventional BLC has a narrow bandwidth. A multi-section BLC configuration with loading stub elements as shown Fig. 1 (c), has different degrees of freedom to be optimized it for wideband operation [16]. The feeding BLC is printed on a substrate RO3003 with thickness $L_3 = 0.25$ mm. Table 1 shows the optimized dimensions of the designed BLC and the stacked antenna.

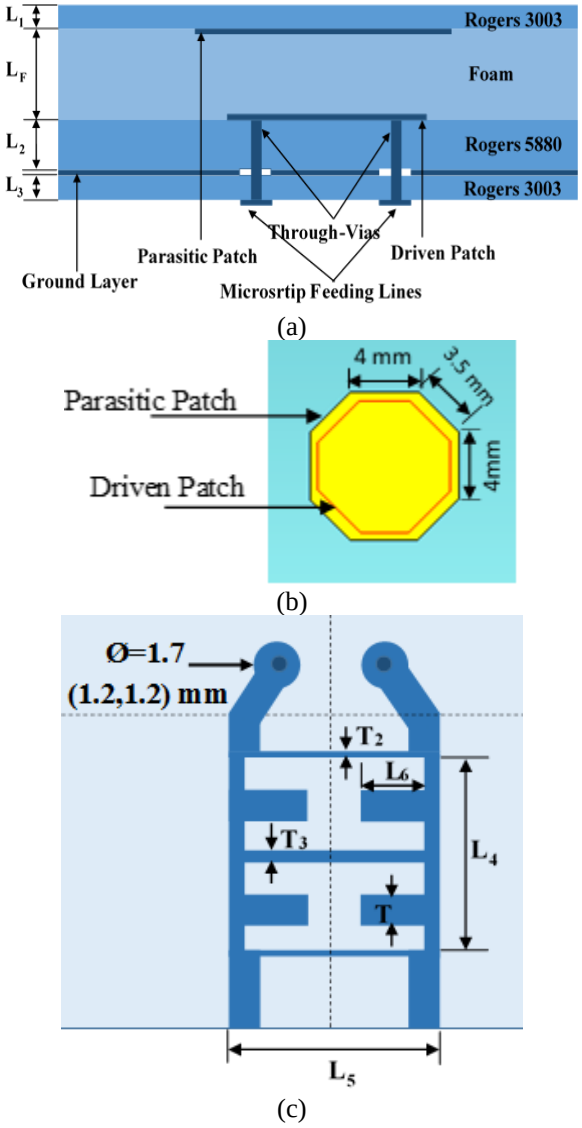

Fig. 1. Geometry of the wideband dual circular polarized antenna element: (a) the side view of the complete antenna element, (b) proposed octagonal patches, and (c) microstrip feeding branch line coupler.

Table 1: Dimensions of the branch line coupler

Parameters	Values (mm)
L4	4.95
L5	5.28
L6	1.2
T	0.9
T2	0.3
T3	0.6

Figure 2 shows the reflection coefficient of the designed octagonal radiating element. The optimized dimensions of the parasitic octagonal patches have vertical and horizontal edges of 4 mm and tilted edges of 3.5 mm. While, the fed octagonal patch have vertical and horizontal edges of 3 mm and tilted edges of 2.5 mm. Due to the symmetry of the designed antenna structure, the reflection coefficients of the two ports are identical. The obtained reflection coefficient of the single element is below -20 dB over all the required bandwidth. Figure 3 shows the axial ratio of the radiated fields in the broadside direction. The obtained axial ratio is below 2dB in the entire operating band.

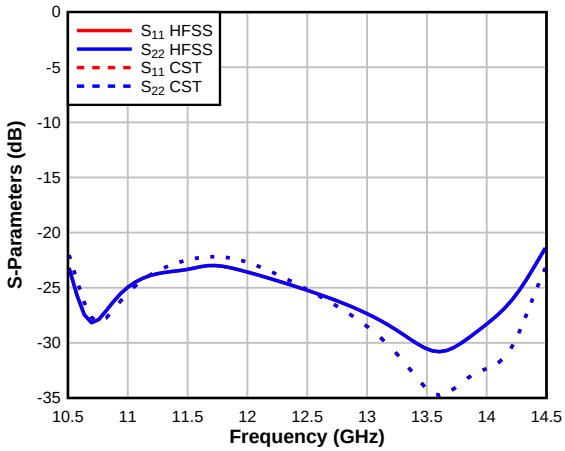

Fig. 2. Reflection coefficient of the single element.

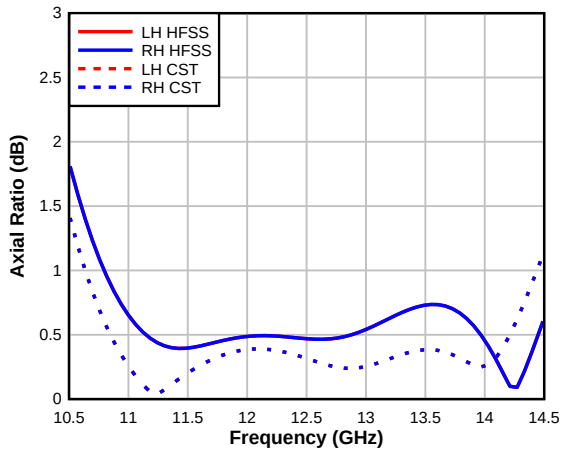

Fig. 3. Axial ratio of the single element.

III. ANALYSIS AND DESIGN OF 4×4 SEQUENTIAL FED DUAL CIRCULAR POLARIZED ANTENNA

The 4 × 4 sub-array is divided into four identical 2×2 sub-cells as shown in Fig. 4. The basic idea of a dual sequential feeding network is to rotate the radiating elements by steps of 90° in addition to changing the phase between the radiating elements by ±90° in a sequential form to obtain LH or RH circular polarization. This sequential feeding mechanism improves the

circular polarization characteristics of antenna array. The key point in the design of such sequential feeding network is to maintain the required phase shifts along the required operating bandwidth. The proposed sequential feeding network is composed of Wilkinson power dividers and appropriate delay lines to introduce the required phase shift. The spacing between the radiating elements is assumed to be 18 mm (0.75 λ_0 at the center frequency) as shown in Fig. 4.

This spacing would introduce a 4×4 array of size 72×72 mm^2 which satisfy the required dimensions of the sub-array for a complete antenna array for Ku-band satellite communication. However, the spacing between the elements is not sufficient to use straight lines for the required phase shifts. Thus, different bends are used to introduce the required lengths of delay lines. In addition, for practical implementation, it is required to add pads for the connectors which would be used to feed this sub-array as shown in Fig. 4. To obtain accurate simulation results, these pads should be included in the simulation.

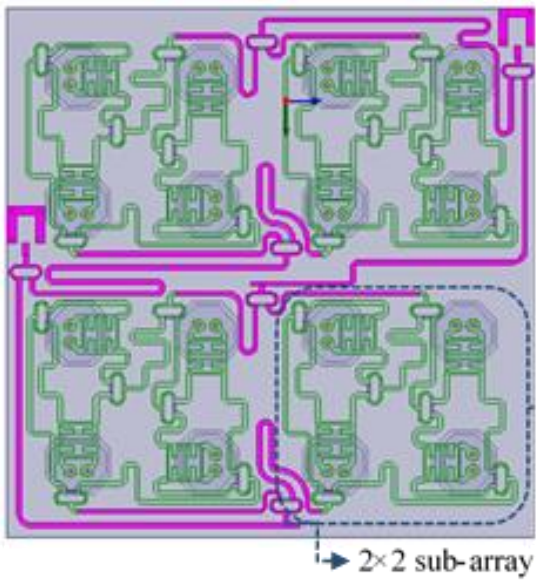

Fig. 4. Sequential feeding network for dual circularly polarized 4×4 radiating elements.

IV. EXPERIMENTAL RESULTS

In this section the experimental results of the designed 4×4 sequential fed antenna array are presented. Figure 5 shows the fabricated antenna structure. Figure 6 shows the used measurement setup inside an anechoic chamber Inc. Model (NSI) 7005-30. Figure 7 shows the measured reflection coefficients for the two excitation ports of both LH and RH circular polarizations together with the simulated results. It can be noted that the measured reflection coefficients satisfy the required specifications to be less than -10dB over the entire operating frequency band. Figure 8 shows the radiation patterns for both RH and LH excitations at 12.7 GHz. The obtained peak gain is around 17 dBi. It can be noted that the cross-polarized component is less than -20dB compared to the co-polarized in the broadside directions for both RH and LH cases. Figure 9 shows the measured and simulated axial ratios for the two circular polarizations as a function of frequency. It can be noted that the measured results satisfy the condition of axial ratio to be less than 3dB for both LH and RH circular polarizations on almost entire operating frequency band. According to the measured results, it can be concluded that the designed dual sequential feeding network introduces the required specifications of matching and radiation properties in the required operating frequency band.

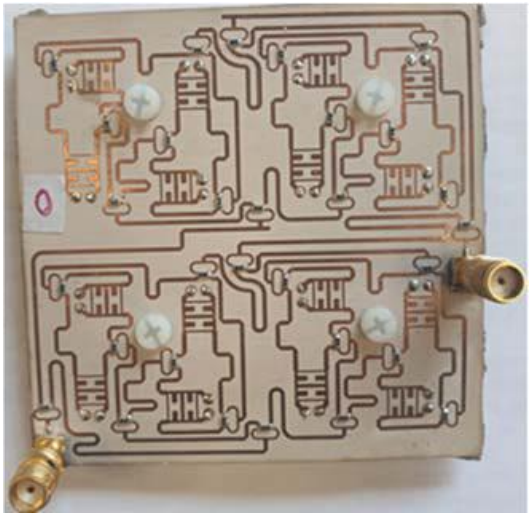

(a)

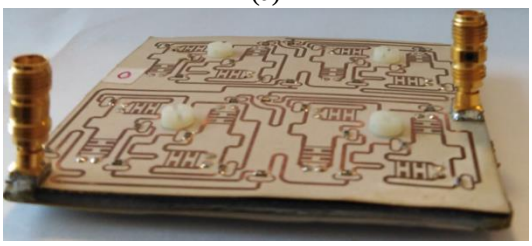

(b)

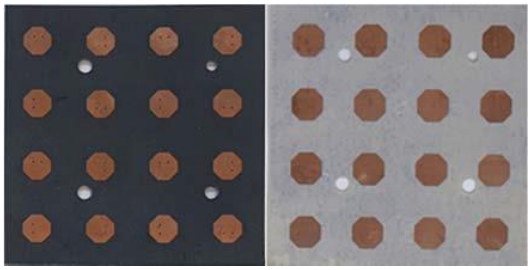

(c)

Fig. 5 Fabricated 4×4 sequential fed antenna: (a) bottom side, (b) side view, and (c) driven and parasitic octagonal patches.

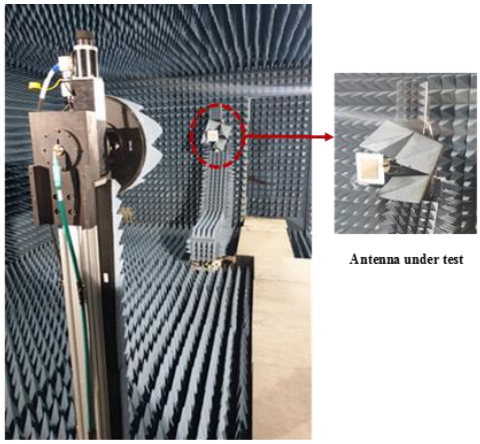

Fig. 6. Measurement setup of the fabricated antenna.

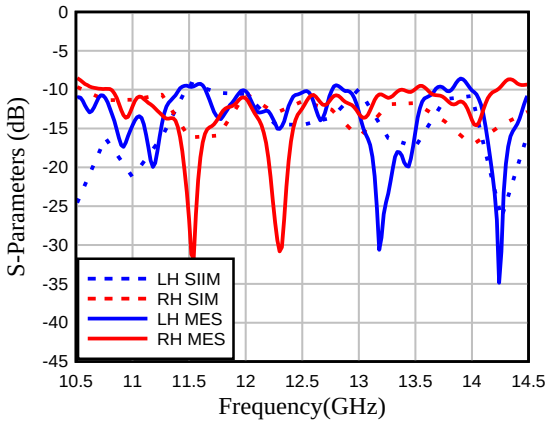

Fig. 7. Measured and simulated reflection coefficient of the 4×4 sequential fed antenna for LH and RH circular polarizations.

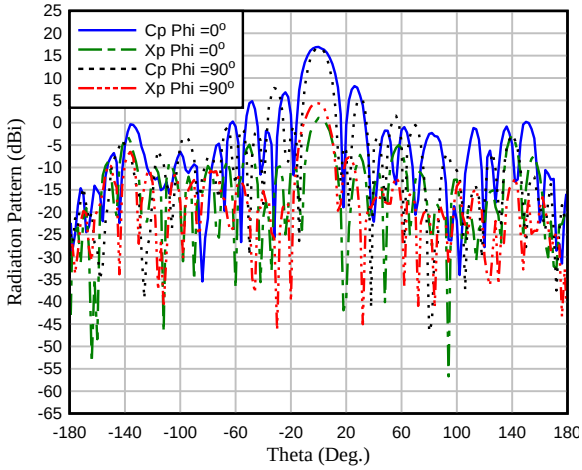

(a)

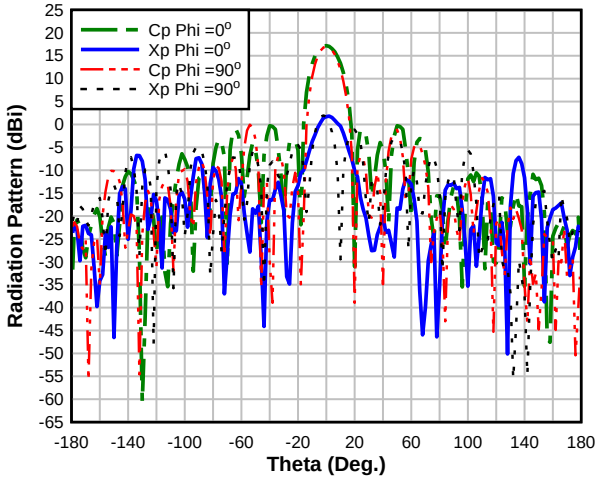

(b)

Fig. 8. Measured radiation patterns for: (a) RH and (b) LH circular polarizations at 12.7 GHz.

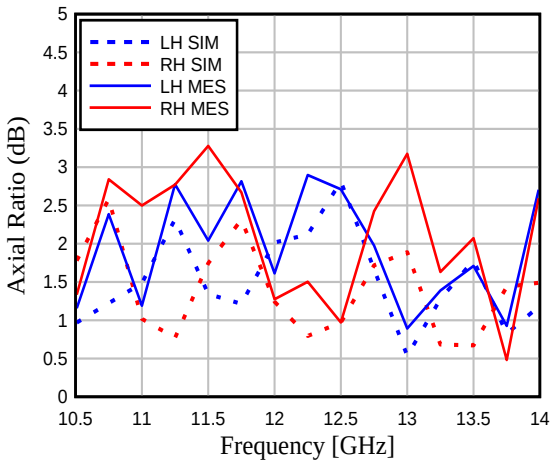

Fig. 9. Measured and simulated axial ratio of the 4×4 sequential fed antenna for LH and RH circular polarizations.

Table 2 shows a comparison between the proposed antenna and previously published configurations for circularly polarized antenna arrays. Based on this comparison, it can be noted that the main advantage of the proposed antenna is the wider bandwidth compared to other configurations. In addition, the antennas in [9-12] are single circularly polarized antennas while the proposed antenna is dual circularly polarized. On the other hand, the antenna in [13] has a quite narrow operating bandwidth compared to the proposed antenna.

Table 2: Comparison between the proposed antenna and previously published antennas

Ref.	No. of Layers	Feeding Technique	Operating Bandwidth (GHz)
[9]	Single layer	Circularly Polarized Microstrip antenna with simplified feed network	9.8 – 11.23
[10]	Single layer	Circularly Polarized 2×2 patch array using a sequential-phase feeding network	5.20 – 6.23
[11]	Single layer	Circularly Polarized Uniform Transmission Lines Using Sequential-Phase Feed	2.08 – 2.95
[12]	Single layer	Circularly Polarized Slotted Substrate Integrated Waveguide Antenna Arrays	11.95 – 12.95
[13]	Multi-layer	Dual Circularly Polarized double-sided dipole array	Dual Band 8.15 – 8.35 and 14.2 – 14.8
This work	Multi-layer	Dual Circularly Polarized 4×4 stacked circular patches antenna array using Sequential feed	Wide band 10.95 – 14.5

V. CONCLUSION

Design and analysis of a dual sequential feeding network for a dual circularly polarized 4×4 antenna array in Ku-band are presented. The radiating element is composed of a wideband stacked octagonal patches fed by a wideband branch line coupler to introduce the required dual circular polarizations. The radiating elements are arranged in sequential forms of 2×2 elements and connected together by two main feeding networks; one for LH circular polarization and the other for RH circular polarization. The effects of coupling between the different parts of the complete feeding network is compensated by adding appropriate stubs to improve the matching and the axial ratios along the design operating frequency band from 10.5 to 14.5 GHz.

REFERENCES

[1] H.-T. Zhang, W. Wang, M.-P. Jin, and X.-P. Lu., "A dual-polarized array antenna for on-the-move applications in Ku-band," *IEEE-APS Topical Conference on Antennas and Propagation in Wireless Communications (APWC)*, pp. 5-8; Cairns, Australia, 2016.

[2] Methods for the determination of the coordination area around an earth station in frequency bands between 100 MHz and 105 GHz, 2016 Edition of ITU Radio Regulations, vol. 2, Appendix 7, 2016.

[3] H.-T. Zhang, W. Wang, M.-P. Jin, Y.-Q. Zou, and X. Liang, "A novel dual-polarized waveguide array antenna for Ku band satellite communications," *IEEE International Symposium on Antennas and Propagation & USNC/URSI National Radio Science Meeting*, San Diego, California, USA, pp. 633-634, 2017.

[4] M. Akbari, A. Farahbakhsh, and A.-R. Sebak, "Ridge gap waveguide multilevel sequential feeding network for high-gain circularly polarized array antenna," *IEEE Trans. Antennas and Propagation*, vol. 67, no. 10, pp. 251-259, 2019.

[5] G. L. Huang, S. G. Zhou, and T. Yuan, "Design of a compact wideband feed cluster with dual-polarized sum-and difference-patterns implemented via 3-D metal printing," *IEEE Trans. Industrial Electronics*, vol. 65, no. 9, pp. 7353-7362, 2018.

[6] M. K. Verma, B. K. Kanaujia, J. P. JSaini, and P. Saini, "A novel circularly polarized gap-coupled wideband antenna with DGS for X/Ku-band applications," *Electromagnetics*, vol. 39, no. 3, pp. 186-197, 2019.

[7] S. Liu, K. Jiang, G. Xu, X. Ding, K. Zhang, J. Fu, and Q. Wu, "A dual-band shared aperture antenna array in Ku/Ka-Bands for beam scanning applications," *IEEE Access*, 7, pp. 78794-78802, 2019.

[8] A. Harrabi, T. Razban, Y. Mahe, L. Osman, and A. Gharsallah, "Theoretical approach for the design of a new wideband Ku-band printed antenna," *Applied Computational Electromagnetics Society Journal*, vol. 30, no. 11, pp. 1200-1208, 2015.

[9] T. Sallam and A. M. Attiya., "Different array synthesis techniques for planar antenna array," *Applied Computational Electromagnetics Society Journal*, vol. 34, no. 5, pp. 716-723, 2019.

[10] Y. Zou, H. Li, Y. Xue, and B. Sun, "A high-gain compact circularly polarized microstrip array antenna with simplified feed network," *Int. J. of RF Micro. Comput. Aided Eng.*, e21964, 2019.

[11] C. Deng, Y. Li, Z. Zhang, and Z. Feng, "A wideband sequential-phase fed circularly polarized

patch array," *IEEE Trans. Antennas and Propag.*, vol. 62, no. 7, pp. 3890-3893, 2014.

[12] S.-K. Lin and Y.-C. Lin, "A compact sequential-phase feed using uniform transmission lines for circularly polarized sequential-rotation arrays," *IEEE Trans. Antennas and Propag*., vol. 59, no. 7, pp. 2721-2724, 2011.

[13] R. Kazemi, S. Yang, S. H. Suleiman, and A. E. Fathy, "Design procedure for compact dual-circularly polarized slotted substrate integrated waveguide antenna arrays," *IEEE Trans. Antennas and Propag.*, vol. 67, no. 6, pp. 3839-3852, 2019.

[14] Ansoft High Frequency Structure Simulator (HFSS) ver. 14, Ansoft Corp., 2014.

[15] CST Microwave Studio, ver. 2012, Computer Simulation Technology, Framingham, MA, 2012.

[16] J. Zhu, Y. Yang, S. Li, S. Liao, and Q. Xue, "Dual-band dual circularly polarized antenna array using FSS-integrated AMC ground for vehicle satellite communications," *IEEE Trans. Vehic. Tech.*, vol. 68, no. 11, pp. 10742-10751, 2019.

[17] C. A. Balanis, *Antenna Theory: Analysis and Design*. John Wiley & Sons, 2016.

[18] M. Mahajan, S. K. Khah, and T. Chakravarty, "Extended cavity model analysis of stacked circular disc," *Progress in Electromagnetics Research*, vol. 65, pp. 287-308, 2006.